RESEARCH ARTICLE

Synergetic effect of Leucophyllum frutescens and Ehretia microphylla dyes in enhancing the photovoltaic performance of dye-sensitized solar cells

Amutha Soosairaj[1] · Ahalya Gunasekaran[2] · Sambandam Anandan[2] · Leo Rajesh Asirvatham[1]

Abstract

The use of new natural dyes derived from *Leucophyllum frutescens* and *Ehretia microphylla* as well as their combination in dye-sensitized solar cells (DSSCs) has been explored for the first time in the current work. The primary pigments that sensitize the semiconductor TiO_2 films were found to be carotenoid, anthocyanin, and chlorophyll. Pigments from *Leucophyllum frutescens* and *Ehretia microphylla* were designated as LF and EM, and their mixture blended at volume percent of 50:50, 75:25, and 25:75 were labeled as LE1, LE2, and LE3, respectively. The absorption range, emission intensities, and the functional groups of the dyes and dye-loaded TiO_2 photo-anode films were analyzed using ultraviolet-visible, photoluminescence and Fourier transform infrared spectroscopy. The surface morphology of bare and sensitized TiO_2 films was identified through scanning electron microscopy (SEM). To evaluate the photovoltaic performance of the fabricated devices, the current-voltage characteristics, electrochemical impedance spectroscopy analysis and incident photon-to-current conversion efficiency measurements were performed. The study found that the co-sensitized cell LE2 outperformed both single and mixed dye-based cells, achieving a maximum conversion efficiency of 1.33% with a V_{oc} of 516 mV and a J_{sc} of 2.55 mA cm^{-2}. This synergetic effect of natural dyes proved the superior performance of DSSCs with co-sensitization.

Keywords DSSC · Natural sensitizers · *Leucophyllum frutescens* · *Ehretia microphylla* · Co-sensitization · Current conversion efficiency

Introduction

Fossil fuels, which are widely employed in all energy sectors, are quickly running out due to overuse. Excessive burning of fossil fuels causes environmental havoc, like global warming, climate change, and ozone depletion. Certain alternative, sustainable, and easily accessible energy sources, like solar energy, are required to address such pressing challenges. In the past score of years, research on dye-sensitized solar cells (DSSCs) has advanced significantly, yielding certain promising results (Mariotti et al. 2020). The first DSSC was developed by Gratzel and O' Regan in 1988. DSSCs offer technically and financially viable alternatives to traditional solar cell technology (O'Regan and Grätzel 1991). Since its invention, a number of initiatives have been made to improve the performance of DSSCs, including the development of effective sensitizers, alternative redox couples, and the preparation of cathode and photo-anode (Castillo-Robles et al. 2021). The current research focuses on dye molecules that play an essential role as sensitizers in the performance of DSSCs (Anoua et al. 2021b). The widely used sensitizers in DSSC applications are transition metal coordination compounds based on ruthenium and porphyrin dyes that can achieve higher efficiencies by up to 13% (Sowmya et al. 2021). However, this type of dye molecules is not ideal due to their lack of cost efficiency, scarcity in nature, substantial environmental impact, and expensive synthesis process (Surana et al. 2021).

✉ Leo Rajesh Asirvatham
aleorajesh@gmail.com

1 Department of Physics, St. Joseph's College (Autonomous), Affiliated to Bharathidasan University, Tiruchirappalli 620002, India

2 Nanomaterials and Solar Energy Conversion Lab, Department of Chemistry, National Institute of Technology, Tiruchirappalli 620 015, India

Natural pigments are viewed as promising alternatives to synthetic dyes in DSSCs due to their simple preparation method, low-cost efficiency, total biodegradable nature, ease of availability, and environmental friendliness (Anoua et al. 2022). When compared to commercial synthetic dyes, natural dyes do suffer from certain disadvantages, namely poor photovoltaic performance and short-term stability (Mariotti et al. 2020). According to Anoua et al., the Curcuma longa-based natural DSSC, using physical vapor deposition, yielded 0.86% of efficiency (Anoua et al. 2021a). Ajaz et al. fabricated a DSSC with Carissa spinarum berry extract that provided 0.95% efficiency (Ajaz et al. 2022). It is reported that the DSSC's conversion efficiency increases with the combination of natural dyes through the co-sensitization process (Patni et al. 2020). Kabir et al. developed DSSCs by combining natural dyes from Malabar and red spinach that gained an optimized cell efficiency of 0.847% (Kabir et al. 2019). Ezike et al. fabricated DSSCs with chlorophyll and anthocyanin co-sensitizers which attained 1.14% efficiency (Ezike et al. 2021).

In the present research, DSSCs are fabricated using two natural plant-based dyes from *Leucophyllum frutescens* flowers and *Ehretia microphylla* leaves and attained the highest efficiency of 1.33% through the co-sensitization process. *Leucophyllum frutescens* is a perennial bedding shrub from the *Scrophulariaceae* family that can endure summer heat and drought stress. Although it is native to Texas and Mexico, it is now widely cultivated in South Asia where it flowers magnificently in steamy tropical weather. It has silver green leaves and purple bell-shaped flowers (Younis et al. 2017). *Ehretia microphylla* belongs to the *Boraginaceae* family that is widely available in tropical South Asian countries (Sharma et al. 2022). The first reason for choosing *L. frutescens* and *E. microphylla* in the current research work is to fabricate environmentally benign DSSCs using widely available plants in southern regions of India. The second reason is that anthocyanin and carotenoid pigments are present in *L. frutescens* as well as flavonoid and chlorophyll pigments are present in *E. Microphylla*. Moreover, these natural dyes are not employed as sensitizers in any of the reported DSSCs so far.

Therefore, the current research is unique since it combines *L. frutescens* and *E. microphylla* as co-sensitizers to enhance the photovoltaic performance of DSSCs. The optical behavior of the individual and combined dyes is obtained through ultraviolet-visible (UV-Vis) spectroscopy, and the emission spectra are recorded using photoluminescence spectroscopy (PL). Fourier transform infrared spectroscopy (FTIR) is used to analyze the functional groups that are present in the dyes. Scanning electron microscopy (SEM) is used to examine the density and uniformity of the dye pigments on TiO_2 films. These results validate the dye molecules as effective sensitizers in the fabrication of dye-sensitized solar cells. The essential photo electrochemical parameters for the DSSCs, such as short circuit current density (J_{sc}), open circuit voltage (V_{oc}), fill factor (FF), and conversion efficiency (η) are investigated through I–V characteristic measurements under standard air mass 1.5 illumination (85 mW cm^{-2}). The electrochemical impedance (EIS) and incident photon-current conversion efficiency analysis (IPCE) are performed to study the charge transport property and quantum conversion efficiency of the fabricated solar cells.

Experimental

Materials

Fluorine-doped tin oxide (FTO) conducting glass (resistivity 7 Ω/sq., transmittance > 80%), TiO_2 powder (anatase, particle size ~ 25 nm), Triton X-100, polyethylene glycol (PEG, M.W 10,000), ethanol, hydrochloric acid (HCL), nitric acid, potassium iodide (KI), iodine (I_2), and $H_2[Pt(Cl)_6]$ were purchased from Sigma Aldrich.

Preparation of TiO_2 paste and photoanode

FTO conductive glass sheets were cleaned in an ultrasonic bath with a detergent solution for 15 min, then rinsed with diluted HCL, ethanol and distilled water and left to air dry. The doctor blade approach was used to make the TiO_2 photoanode (Khammee et al. 2021). TiO_2 homogeneous paste was prepared by combining and blending 0.2 g of TiO_2 powder, 0.4 ml of (0.1 M) nitric acid solution, and 0.08 g of polyethylene glycol. The colloidal solution was mixed with the non-ionic surfactant Triton X-100 (0.05 ml), milled for 30 min, and then kept in an ultrasonic bath for an hour. To set the active area as 25 mm^2, adhesive tape was used on the conductive side of FTO substrates (5 mm × 5 mm). A few drops of TiO_2 suspension were applied to the edge of the substrate, and a glass rod was used to spread the paste evenly across the FTO. The coated plates were air dried and sintered for 2 h at 450 °C in a hot plate.

Preparation of counter electrode and electrolyte

Platinum coated counter electrodes were prepared by drop-casting (4 mM) of $H_2[Pt(Cl)_6]$ in a pre-cleaned FTO plate, followed by sintering at 450 °C for 30 min (Gunasekaran et al. 2020). I^-/I_3^- redox couple served as liquid electrolyte in the construction of DSSCs. For the preparation of the electrolyte solution, 0.83 g of potassium iodide (KI) and 0.127 g of iodine (I_2) were dissolved in 10 ml of ethylene glycol (Hossain et al. 2017). The liquid electrolyte solution was then collected in a black bottle and stored in a dark place away from direct sunlight.

Preparation of sensitizers

Natural purple and green dyes were extracted from *Leucophyllum frutescens* (LF) flowers and *Ehretia microphylla* (EM) leaves, respectively. The flowers and leaves were washed thoroughly with distilled water and air dried for 30 min. They were cut into small slices and placed in 100 ml of ethanol solution for 24 h without direct exposure to sunlight. Finally, the solid residues were filtrated out using Whatman filter paper and stored in a dark place for further use as sensitizers in DSSC. Combining these two dyes at different volume ratios, three different combinations of dyes (purple + green) were prepared.

LF → 30 ml purple dye (100% purple)
EM → 30 ml green dye (100% green)
LE1 → 15 ml purple dye + 15 ml green dye (1 : 1)
LE2 → 20 ml purple dye + 10 ml green dye (2 : 1)
LE3 → 10 ml purple dye + 20 ml green dye (1 : 2)

Fabrication of DSSC

TiO_2 electrodes were heated to 80 °C and immersed in the dye solutions of LF, EM, LE1, LE2, and LE3 for 24 h (Ramamoorthy et al. 2016). In order to assemble the DSSCs, the platinum counter electrode and dye-stained TiO_2 photoanode were placed facing each another and clipped together with binder clips. A few drops of electrolyte solution were applied on the edge of the plate and allowed to diffuse by capillary action between the plates.

## Characterization and measurements

The UV–visible absorption spectra of single, mixture dyes, and sensitized films were recorded using a UV–visible spectrophotometer (Perkin Elmer Lambda 35). Photoluminescence analysis was done by fluorescence spectrophotometer (Perkin Elmer LS 45). The FTIR spectra for dye molecules were measured through FT-IR spectroscopy (Perkin Elmer spectrum RX-1). The surface morphology of TiO_2 and the sensitized films was done using scanning electron microscopy (CAREL ZEISS EVO-18). The photovoltaic measurement of DSSCs was performed under 85 mWcm^{-2} light illumination with an Oriel 150 W Xe light source solar simulator to measure the photovoltaic properties of the cells. The AUTOLAB12/FRA2 electrochemical analyzer was used for measuring the electrochemical properties of the cells. Enlitech QE-T spectral equipment was employed to measure the incident photon to current conversion efficiency (IPCE) of the fabricated DSSCs.

Results and discussions

Optical studies

Solution spectra of dyes

The optical absorption spectra of the individual and combined dyes of *Leucophyllum frutescens* and *Ehretia microphylla* are obtained in the visible region from 400 to 700 nm as shown in Fig. 1a. In the spectra of the LF extract, the first major peak appearing at 476 nm signifies the presence of carotenoid with a range of 452 to 487 nm (Azevedo-Meleiro and Rodriguez-Amaya 2004) (Ardy et al. 2020) (Rodríguez et al. 2017) and another major
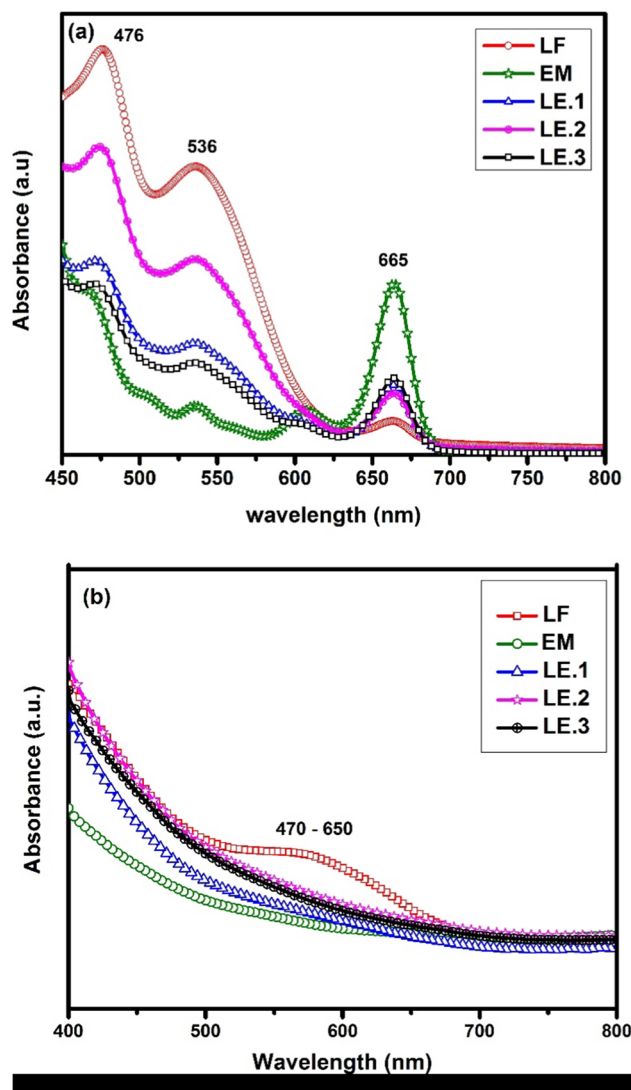
Fig. 1 Absorption spectra of **a** LF, EM, LE1, LE2, and LE3 dyes. **b** LF, EM, LE1, LE2, and LE3 dye-sensitized TiO_2 films

peak appearing at 536 nm with the spectrum range of 517 to 552 nm confirms the presence of anthocyanin (Inbarajan et al. 2022) (Ayalew and Ayele 2016) (Ahmad et al. 2020). Besides, a minor peak is found at 665 nm with less intensity indicating the presence of chlorophyll. In the spectra of the EM extract, a significant absorption peak appearing at 665 nm with the spectrum range of 634 to 681 nm reveals the presence of chlorophyll (Noor et al. 2014) (Zhou et al. 2011). There are two other, less prominent minor peaks found at 476 and 536 nm in the EM spectrum which are associated to carotenoid and anthocyanin pigments. As was already mentioned, the pigments of both LF and EM extracts are present in LE1, LE2, and LE3 co-sensitized extracts in different ratios. As a result, the primary peaks associated with LF and EM are seen together in LE1, LE2, and LE3 spectra, at 476, 536, and 665 nm with different intensities. The first peak at 476 confirms the presence of carotenoid; the second peak at 536 nm confirms the presence of anthocyanin, and the third peak at 665 nm is attributed to the presence of chlorophyll.

From the spectra of co-sensitizers, it is evident that LE2 has a higher absorption intensity than LE1 and LE3 due to its high mixture of LF belonging to carotenoid and anthocyanin pigments. Given that DSSCs primarily rely on the broad absorbing ability of the dyes, the wide spectrum of LE2 with high intensity could effectively contribute to the conversion efficiency of DSSCs compared to other combination dyes. The extracts of LE1, LE2, and LE3 show that the combined dye has a greater and wider spectrum of absorption than the individual dye.

Film spectra of the sensitized photoanode

The LF, EM, LE1, LE2, and LE3 dye-sensitized photoanodes have almost identical pattern as shown in Fig. 1b. However, the LF extracted dyes adsorbed on TiO_2 film have a bulge around 470 to 650 nm, indicating strong adherence of the dye to TiO_2 film. Furthermore, for LE1, LE2, and LE3 photoanodes, the absorption is governed until 800 nm suggesting that by sensitizing TiO_2 with the mixture of dyes the light absorption range could be enhanced and become favorable in light harvesting. The intensity of the co-sensitized dye LE2 is slightly higher than LF at 400 nm and again at 675 to 800 nm. The efficient sensitization of co-sensitized dye with TiO_2 molecules is confirmed by the higher intensity absorption of LE2 than LE1, LE3, and EM films in the visible range. The EM film shows less absorption in the visible region due to weak binding with TiO_2 (Dhafina et al. 2020). The absorption spectra reveal that the cocktail dyes increase the range of the absorption wavelength which in turn increases the photoelectric conversion efficiency of DSSC.

Photoluminescence spectra analysis

Solution spectra

In the process of photoluminescence, a chemical compound absorbs a photon, transitions to a higher electronic energy state and returns to a lower energy state by radiating a photon (Prabu et al. 2021). In Fig. 2a, the emission spectra of LF, EM, LE1, LE2 and LE3 dyes are recorded in the range of 550 to 900 nm under excitation at 450 nm wavelength. For LF, LE1, LE2, and LE3 extracts, the emission peaks emerged at 670 and 726 nm with varying intensities. Peaks in the red region originate from the recombination of a photo generated hole with a singly ionized electron in the valence band, which causes the red emission of materials. The emission peak at 676 nm with an arm at 725 nm that appeared for EM dye extract indicates the characteristic response of
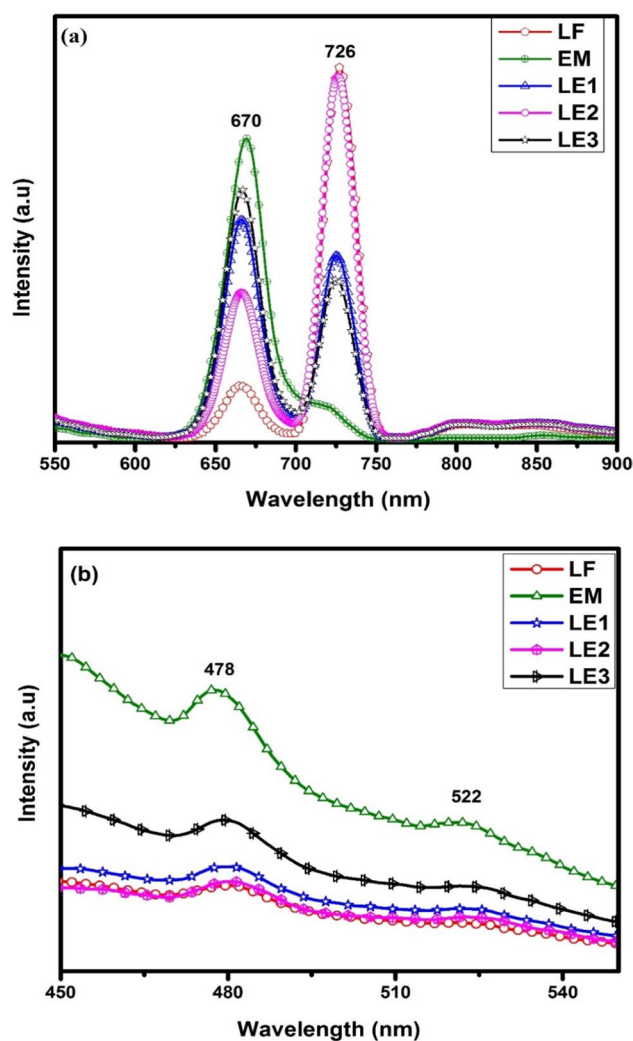
Fig. 2 Emission spectra of **a** LF, EM, LE1, LE2 and LE3 dyes. **b** LF, EM, LE1, LE2, and LE3 dye-sensitized TiO_2 film

chlorophyll. Chlorophyll exhibits a red shift compared to the absorption spectrum. There is no green region emission found in the entire spectra and the intensity of the emission of LF, LE1, LE2, and LE3 extracts exhibits a bathochromic shift compared with that of EM which is the characteristic of chlorophyll in a polar solvent (Adedokun et al. 2018) (Adedokun et al. 2021).

Film spectra

The PL emission spectra of sensitized photo-anodes in Fig. 2b with LF, EM, LE1, LE2 and LE3 dyes are recorded to analyze further characteristics of photo-generated charge carriers such as migration, recombination of photo-generated carrier trapping, separation of the electron-hole pairs, and charge transfer. In the spectra, emission peaks are exhibited at 478 nm and 522 nm for all the films. The spectra confirm that the intensity of the emission peak of LE2 is less than all other sensitized films. Lower PL intensity generally suggests a lower recombination rate, whereas higher PL intensity generally indicates a higher charge carrier recombination rate, which may not be suitable for exhibiting better photocatalytic activities in the photo-anode (Prabhu et al. 2022). A maximum number of free electrons are made available by preventing recombination, allowing for efficient charge transportation. The emission intensity of EM film is higher than all other films, and the peak intensity is gradually decreasing in the sequence of LF, LE1, LE3, and LE2 in the visible region. The PL spectrum of the co-sensitized film LE2 proves to be the ideal photoanode for better light absorption with less emission. The photoemission spectra of sensitized TiO_2 films agree well with the results of optical absorption spectra.

Fourier transform infra-red analysis

The functional groups of the chemically active substances in plant extracts are identified on the basis of their peak values in the infrared radiation region. The nature of the bonds and functional groups of the mono and mixer dyes used in the present work are recorded using FTIR spectroscopy. The FT-IR spectra of LF, EM, LE1, LE2, and LE3 dyes are shown in Fig. 3 with a spectral range of 4000–400 cm^{-1}. An ideal dye must have carboxyl (COOH) or hydroxyl (O-H) anchoring groups to inject electrons effectively into the conduction band (CB) of the semiconductor (Sankaranarayanan et al. 2022). The peaks found at 675 cm^{-1} and 880 cm^{-1} in the solution spectra correspond to C-H bending vibrations. All the dye molecules exhibit peaks at 1040 cm^{-1} with slightly different transmittance intensities that are attributed to C–C vibrations of the tetra pyrrole ring of chlorophyll. This variation of intensities is attributed to the percentage of chlorophyll present in all the pure and mixture of dyes. Since
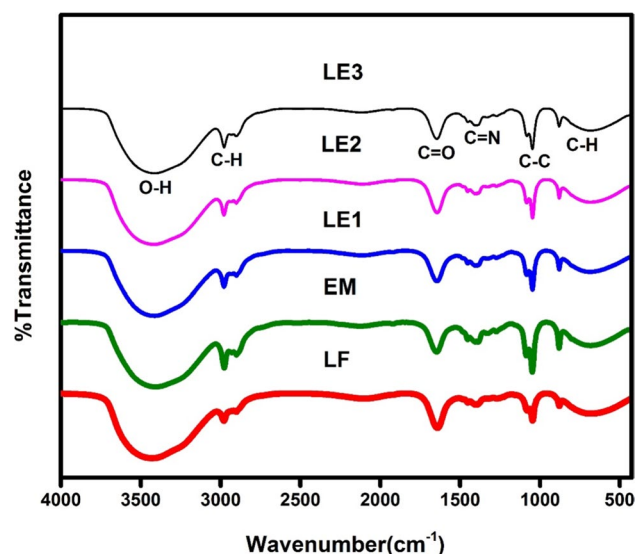

Fig. 3 FT-IR spectra of LF, EM, LE1, LE2 and LE3 dyes

there is a very minimal percentage of chlorophyll in LF, the C–C vibrations are much weaker. However, in EM pigment, the peak at 1040 cm^{-1} is more intense and sharp due to its high chlorophyll content. All the other combination dyes, LE1, LE2, and LE3, have moderate peak intensities at 1040 cm^{-1} because they contain a portion of chlorophyll in them. The emerging peaks at 1645 cm^{-1} strongly support the existence of C=O bonding, while the broad peak between 3000 cm^{-1} and 3700 cm^{-1} corresponds to the intermolecular bonded O–H stretching vibration (Al-Alwani et al. 2018) (Rajkumar et al. 2019). The peak at 1382 cm^{-1} is due to carbon–nitrogen carbon bending and C=N symmetric stretching vibrations. The aromatic CH stretching vibrations are recorded at 2974 cm^{-1}, while the peak of the aliphatic CH group is at 2887 cm^{-1} (Patni et al. 2020). The spectra reveal that no new peak is created by combining the extracted dyes other than very tiny adjustments in the intensity peak positions, proving that the individual pigments do not interact chemically and coexist harmoniously.

Scanning electron microscopy (SEM) analysis

TiO_2 films in the conductive glass of FTO are characterized by SEM analysis to study the cohesion, homogeneity, and porosity of the film. The surface morphology of bare TiO_2 film and dye-sensitized TiO_2 films at different magnifications is investigated in Fig. 4 through scanning electron microscopic images. From Fig. 4a, it is evident that the deposited TiO_2 film is porous, spherical, and homogeneous after annealing at 450 °C, with no surface cracks or fractures. The uniform distribution of the nanoparticles also ensures sufficient dye adsorption and light harvesting. The dye-sensitized films with LF and EM extracts found
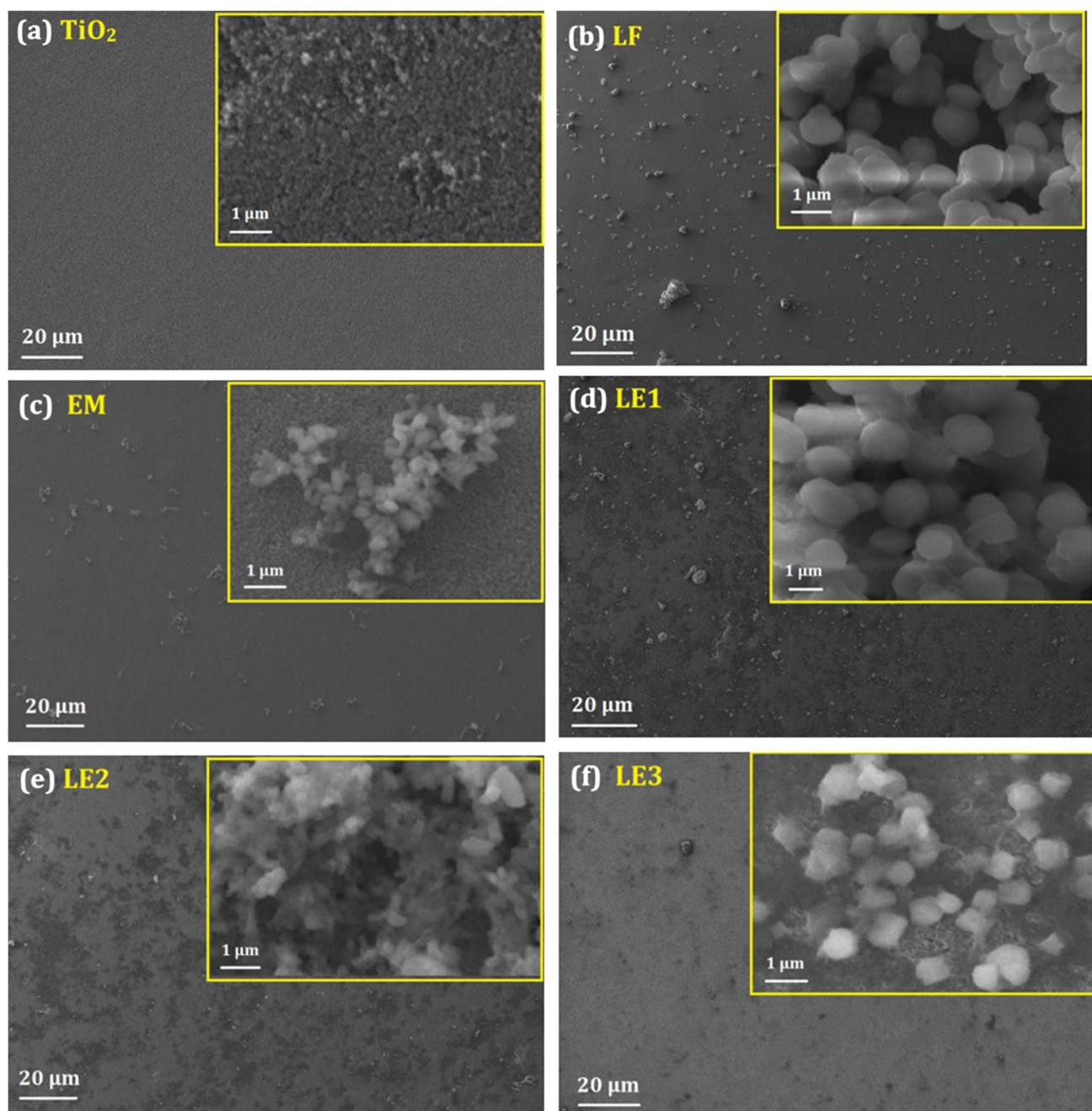
Fig. 4 SEM images of **a** TiO$_2$ film, **b** LF, **c** EM, **d** LE1, **e** LE2, and **f** LE3 loaded TiO$_2$

in Fig. 4b and c show good adhesion on the surface of the TiO$_2$ film. Due to the superior anchoring groups found in anthocyanin and carotenoid, dye pigments in LF (Fig. 4b) are very dense compared to EM (Fig. 4c). Figure 4d, e, and f show co-sensitized LE1, LE2, and LE3 films having both LF and EM pigments together with their volumetric proportion of dye mixture. From Fig. 4d and e, it is clear that LE1 and LE2 pigments are uniformly dispersed and densely packed on TiO$_2$ photo electrodes whereas LE3 sensitized film in Fig. 4f has poor density and homogeneity. This difference in

density and homogeneity of dye pigments in LE1, LE2, and LE3 could be related to the anchoring groups of the respective dyes present in them.

Photo electrochemical behavior of DSSC

Current—voltage characteristics

The photovoltaic performance of the fabricated DSSCs is measured under 85 mW cm^{-2} light at AM 1.5 condition.
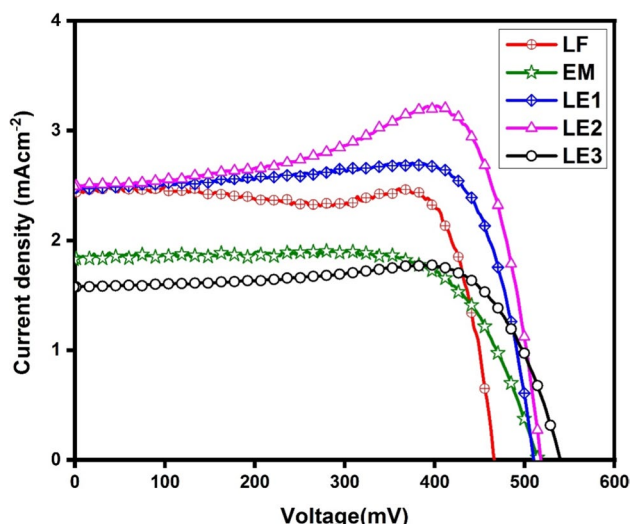
Fig. 5 Photocurrent—voltage curves for LF, EM, LE1, LE2, and LE3 devices

Table 1 Photocurrent—voltage parameters and IPCE measurements of LF, EM, LE1 and LE2 devices

Dye	J_{SC} (mAcm^{-2})	V_{OC} (mV)	FF	η %	IPCE %
LF	2.42	465	0.82	1.08	28.15
EM	1.84	514	0.73	0.81	23.32
LE1	2.46	509	0.84	1.26	31.28
LE2	2.55	516	0.85	1.33	33.89
LE3	1.59	538	0.84	0.84	20.21

Figure 5 illustrates the plotted current density vs voltage. Using LF, EM, LE1, LE2, and LE3 as sensitizers, the photo electrochemical behavior of the DSSCs is expressed in Table 1 in terms of open-circuit voltage (V_{oc}), short-circuit current density (J_{sc}), maximum voltage (V_{max}), maximum current (I_{max}), fill factor (FF), and efficiency (η). Short circuit current density (J_{sc}) is produced and collected from light-generated carriers, whereas open circuit voltage (V_{oc}) is produced in solar cells by the amount of forward bias at the cell junction.

Fill factor reflects the electrochemical and electrical losses that occur during DSSC operation, i.e., ratio of maximum to theoretical power output from solar cell, which is calculated as follows (Calogero et al. 2015):

$$FF = \frac{J_{max} \times V_{max}}{J_{sc} \times V_{oc}} \tag{1}$$

where J_{max} and V_{max} are maximum obtained current and voltage. The capacity of the solar cell is determined by the conversion efficiency. The efficiency is dependent on the intensity of incident light and is calculated as follows (Ludin et al. 2014):

$$\eta(\%) = \frac{J_{sc} \times V_{oc} \times FF}{P_{in}} \tag{2}$$

The dye extracted from *Ehretia microphylla* with chlorophyll pigments (EM) exhibits a cell efficiency of 0.81% with J_{sc} of 1.84 mAcm^{-2}, V_{oc} of 514 mV, and FF of 0.73, while the dye derived from *Leucophyllum frutescens* (LF) with anthocyanin and carotenoid pigments demonstrates a cell efficiency of 1.08% with J_{sc} of 2.42 mA cm^{-2}, V_{oc} of 465 mV, and FF of 0.82. The difference in efficiency of these two cells is due to their dye's capacity to bind on to the TiO$_2$. The increased effectiveness of anthocyanin and carotenoid can be ascribed to the presence of alcoholic groups, which improve the adhesion of dye to the nanostructured TiO$_2$. Among the three co-sensitized cells, LE3 with a combination of 10 ml purple (LF) + 20 ml green (EM) is observed with a cell efficiency of 0.84%, J_{sc} of 1.59 mA cm^{-2}, V_{oc} of 538 mV, and FF of 0.84. This conversion efficiency is better than the EM-based and lower than the LF-based DSSCs. The combined dye-based cell LE1, with LF and EM extracts in a volumetric ratio of 1:1, has 1.26% of efficiency with J_{sc} of 2.46 mA cm^{-2}, V_{oc} of 516 mV, and FF of 0.84. In comparison to all the mono- and co-sensitized DSSCs, the LE2 cell with a 2:1 ratio of LF and EM extract attained the maximum efficiency of 1.33% with J_{sc} of 2.55 mA cm^{-2}, V_{oc} of 516 mV, and FF of 0.85 and proved the synergetic effect of the co-sensitized dyes.

The order of the photovoltaic response of DSSCs increases in the sequence from EM, LE3, LF, LE1, and LE2. This response agrees well with the absorption spectra, which show the absorption intensity of the dyes and films in the same order. It is remarkable that the emission range is similarly well matched to the cell efficiencies achieved, just like with LE2, which has the highest conversion efficiency while having the lowest emission, and other cells in a similar way. The conclusions derived from the surface morphology in Fig. 4 again corroborate the I-V results that the photovoltaic response of DSSCs is good when the dyes are dense, homogenous, and well adhered to TiO$_2$.

Electrochemical impedance spectroscopy analysis

The EIS analysis is a powerful, useful, and non-destructive method for investigating interface properties and electron kinetics in DSSC. Three distinctive semicircles with a frequency range of 10^5 to 0.1 kHz comprise the majority of the EIS of a DSSC. Three semicircles from the Nyquist plot exhibit the impedance of the charge transfer resistance (R_{ct1}) on the Pt counter electrode at high frequency, the charge transport resistance (R_{ct2}) on the TiO$_2$/dye/electrolyte

interface at mid-frequency, and diffusion in the electrolyte at low frequency, respectively.

The high-frequency interception on the real axis can be attributed to the sheet resistance (R_s) of transparent conducting oxides (TCO). Consequently, the overall series resistance of DSSC should consist of four resistance values. Since the same Pt electrodes are utilized in all our studies, here we concentrate on the larger semicircle (R_{ct2}) to investigate the photo-generated electron transport and interfacial capacitance at the TiO_2/dye/electrolyte interfaces (Luo et al. 2009) (Li et al. 2015). The semicircle associated with the electrolyte diffusion process is not recorded in our investigations because it is generally observed at frequencies below 0.1 kHz and demands a longer acquisition period. From the plot, the reduced diameter of the semicircles suggests a decrease in the interface layer resistance and an effective separation of photo-generated electron hole pairs and fast interfacial charge transfer between the TiO_2 matrix and the TCO anode. As expected, the semicircles (R_{ct2}) of the DSSCs show wide variations. Among all the single and co-sensitized DSSCs (Fig. 6), the LE2 mixture solar cell exhibits a lower R_{ct2} value of 180.87 Ω while the DSSC with EM exhibits a higher value of 579.94 Ω. The outcome clearly shows a reduction in the resistance of the interface layer and the resistance of charge transfer on the surface. The R_{ct2} values for LE1, LF, and LE3 dye-based DSSCs are 257.76 Ω, 259.72 Ω, and 506.22 Ω. Comparing the R_{ct2} of LF, EM, LE1, and LE3 DSSCs, the R_{ct2} value of LE2 becomes smaller. The results confirm that the co-sensitization favors electron transfer and reduces the recombination of electrons with dye or back-transfer reaction.

Figure 7 illustrates the Bode plot of DSSCs sensitized with single and mixture dyes. It has two peaks, one in the mid-frequency range and the other in the high-frequency
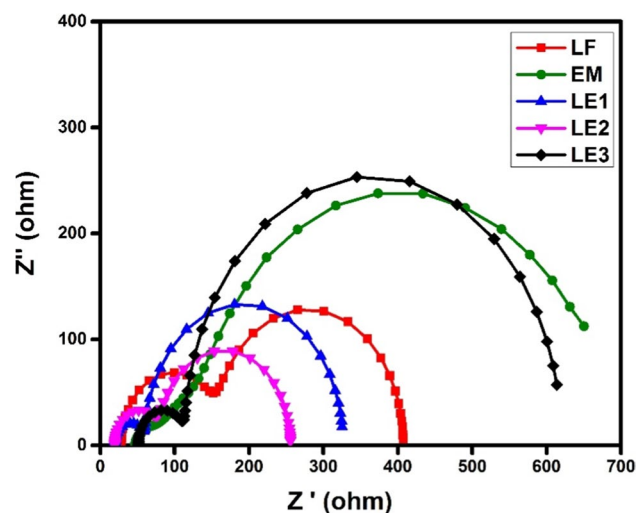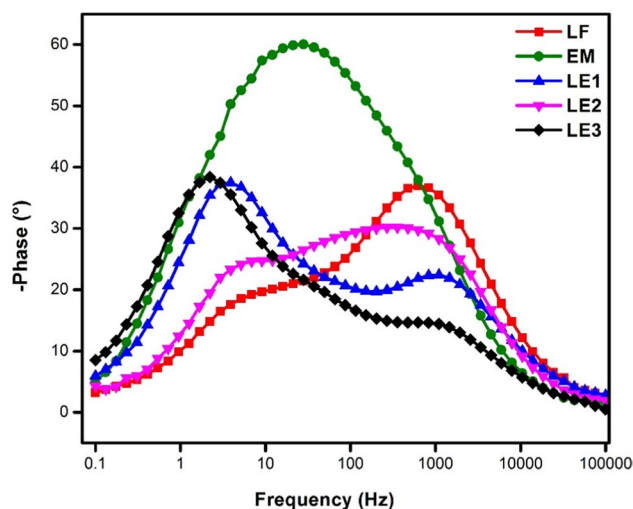

Fig. 7 Bode phase plots of LF, EM, LE1, LE2, and LE3 devices

range which indicate the effective lifetimes of the electrons (Anne Sarah Christinal et al. 2022) on the TiO_2/dye/electrolyte interface and the Platinum counter electrode, respectively.

The peak frequencies are inversely related to the lifetime of an electron. Since the frequency at the high-frequency region is related to the charge transfer at the interface of electrolyte/Pt, the focus is on the characteristic peak at the mid-frequency region, and the obtained values are 35, 58.8, 36.67, 28.96, and 37.53 Hz for LF, EM, LE1, LE2, and LE3 sensitized solar cells, respectively. The lifetime measurement for the DSSCs is calculated using the following formula (Gunasekaran et al. 2020):

$$\tau = \frac{1}{2\pi F} \tag{3}$$

where "τ" is an electron lifetime and "F" is the maximum frequency. The lifetime values obtained from Bode phase plots are given in Table 2. From these values, it is evident that DSSC with LE2 extract has a higher electron lifetime than all other devices which is consistent with I-V and EIS studies. The EM extract suppresses the effective electron hole pair generation in DSSC and gives a lower electron lifetime. The co-sensitized dyes LE1 and LE3 also possess

Fig. 6 Nyquist plots for LF, EM, LE1, LE2, and LE3 devices

Table 2 Photo electrochemical impedance parameters of DSSCs

Dye	R_S(Ωcm^{-2})	R_{CT1}(Ωcm^{-2})	R_{CT2}(Ωcm^{-2})	τ (s)$\times 10^{-3}$
LF	24.41	126.28	259.72	4.54
EM	40.59	36.24	579.94	2.70
LE1	20.37	53.46	257.76	4.34
LE2	13.37	57.59	180.87	5.49
LE3	39.65	70.61	506.22	4.24
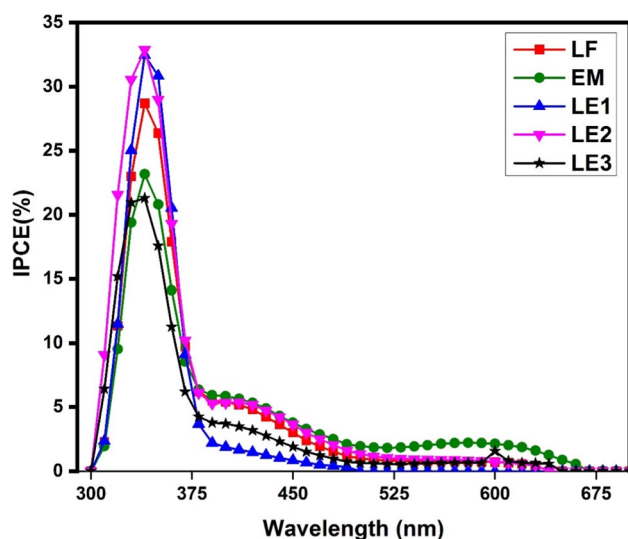
Fig. 8 IPCE spectra of LF, EM, LE1, LE2, and LE3 devices

a higher electron lifetime as that of LF comparably. This is the reason why the co-sensitized dye-based devices produce higher V_{oc} and J_{sc} and higher efficiency than mono dye-based devices.

Incident photon-to-current conversion efficiency (IPCE) analysis

The incident photon-to-current conversion efficiency for the solar cells is illustrated in Fig. 8 in order to assess the efficiency of natural dyes in DSSC performance. The IPCE is calculated by dividing the total number of produced electrons by the total number of incident photons. This value is affected by the light harvesting efficiency and electron transfer yield, which include the injection of a quantum charge and the efficiency of electron capture in the external circuit (Ramamoorthy et al. 2016). The IPCE spectra are shown in the figure as a function of wavelength from 300 to 600 nm. The spectra make it abundantly evident that there is a striking similarity between the IPCE curve and the absorption spectra of specific dyes providing convincing proof that both mono and mixed dye samples show signs of photocurrent conversion. The IPCE values observed at the characteristic wavelengths of the dyes ranged from 20 to 33%, decreasing in the order LE2 > LE1 > LF > EM > LE3. The variance in IPCE values for different natural dyes may indeed be caused by differences in the amount of dye placed onto the TiO_2 thin film, the degree of charge carrier recombination, the energy level of the excited dye molecule, and the quenching of the excited state.

The best energy conversion efficiency is achieved by the co-sensitized dyes LE2, LE1 in the ratios of 2:1 and 1:1, with values of 33.89% and 31.28% at the frequency

range between 310 and 375 nm. The individual dyes LF and EM show a value of 28.15% and 23.32% at the frequency region between 320 and 370 nm. A lower conversion efficiency of 20.21% is exhibited by the mixed dye LE3 between 312 and 368 nm. The results of IPCE are in line with the UV–visible, I–V, and EIS findings, confirming that mixture dye LE2 has a greater conversion efficiency than all other single and mixture dyes. It implies that the synergistic effect in co-sensitization may be a very interesting and effective strategy for further development of naturally dye-sensitive solar cells. From the obtained results of UV-visible absorption, I–V impedance and IPCE measurements, a correlation is found in all of them for LE2 to have a greater photovoltaic response than all other single and mixture of dyes.

Conclusion

The fabricated DSSCs based on single and mixed dyes from *Leucophyllum frutescens* and *Ehretia microphylla* were presented in the current research. The findings revealed that DSSCs based on LE2 cosensitized extract had the highest photovoltaic performance of 1.33% in comparison to other single and mixed dye extracts due to its low charge transfer resistance and broader photo-absorption in the visible range. This result showed that co-sensitization of carotenoid and anthocyanin with chlorophyll at a volume ratio of 2:1 improved the overall efficiency of the cell due to an increase in binding sites and led to an increase in conjugation. The DSSC based on EM extract had the least photovoltaic performance among all the devices with efficiency of 0.81%. The success of the device performance employing the dye combination of carotenoid, anthocyanin, and chlorophyll pigments proved that co-sensitization could be an extremely promising and effective technique for further improvement in natural DSSCs. Although the photovoltaic performance of natural sensitizers is typically lower than that of commercial dyes, they exhibit superior economic and environmental benefits. This consistently arouses a great deal of interest in the research community to continue with natural dye molecules to enhance the performance of the cell and eventually replace the widely used toxic commercial synthetic dye.

Declarations

Ethical approval Not applicable

Consent to participate Not applicable

Consent for publication Not applicable

Competing interests The authors declare no competing interests.

References

Adedokun O, Adedeji OL, Bello IT et al (2021) Fruit peels pigment extracts as a photosensitizer in ZnO-based dye-sensitized solar cells. Chem Phys Impact 3:100039. https://doi.org/10.1016/j.chphi.2021.100039

Adedokun O, Sanusi YK, Awodugba AO (2018) Solvent dependent natural dye extraction and its sensitization effect for dye sensitized solar cells. Optik 174:497–507

Ahmad I, Ahmad S, Rao H et al (2020) Multi-method determination of antioxidant capacity, phytochemical and biological investigation of four different solvent extractives of Leucophyllum frutescens. Environ Sci Pollut Res 1–8

Ajaz P, Feroz A, Mir A (2022) Photovoltaic response of Carissa spinarum berry extract in dye - sensitized solar cell. Environ Sci Pollut Res 1–8. https://doi.org/10.1007/s11356-022-21584-1

Al-Alwani MAM, Ludin NA, Mohamad AB et al (2018) Application of dyes extracted from Alternanthera dentata leaves and Musa acuminata bracts as natural sensitizers for dye-sensitized solar cells. Spectrochim Acta A Mol Biomol Spectrosc 192:487–498

Anne Sarah Christinal R, Prakash I, Chakravarty S, Leo Rajesh A (2022) Spray pyrolysed Cu2ZnSnS4 thin film photovoltaic cell fabricated using cost effective materials. Phys B Condens Matter 637:413911. https://doi.org/10.1016/j.physb.2022.413911

Anoua R, Lifi H, Touhtouh S et al (2021a) Optical and morphological properties of Curcuma longa dye for dye-sensitized solar cells. Environ Sci Pollut Res Int 28:57860–57871. https://doi.org/10.1007/s11356-021-14551-9

Anoua R, Touhtouh S, El Jouad M et al (2021b) Optical and electronic properties of the natural alizarin dye: theoretical and experimental investigations for DSSCs application. Opt Mater (Amst) 127:111347. https://doi.org/10.1016/j.optmat.2021.111347

Anoua R, Touhtouh S, El Jouad M et al (2022) Absorbance and photoluminescence study of pomegranate for dye-sensitized solar cells. Mater Today Proc 66:109–111. https://doi.org/10.1016/j.matpr.2022.03.677

Ardy T, Purnomo B, Steven Y, Febriana R (2020) Selection of maceration solvent for natural pigment extraction from red fruit (Pandanus conoideus Lam) Indones. J Nat Pigment 2(1):8–8. https://doi.org/10.33479/ijnp.2020.02.1.8

Ayalew WA, Ayele DW (2016) Dye-sensitized solar cells using natural dye as light-harvesting materials extracted from Acanthus sennii chiovenda flower and Euphorbia cotinifolia leaf. J Sci Adv Mater Devices 1:488–494. https://doi.org/10.1016/j.jsamd.2016.10.003

Azevedo-Meleiro CH, Rodriguez-Amaya DB (2004) Confirmation of the identity of the carotenoids of tropical fruits by HPLC-DAD and HPLC-MS. J Food Compos Anal 17:385–396. https://doi.org/10.1016/j.jfca.2004.02.004

Calogero G, Bartolotta A, Di Marco G et al (2015) Vegetable-based dye-sensitized solar cells. Chem Soc Rev 44:3244–3294. https://doi.org/10.1039/C4CS00309H

Castillo-Robles JA, Rocha-Rangel E, Ramírez-De-león JA et al (2021) Advances on dye-sensitized solar cells (DSSCs) nanostructures and natural colorants: a review. J Compos Sci 5:1–25. https://doi.org/10.3390/jcs5110288

Dhafina WA, Daud MZ, Salleh H (2020) The sensitization effect of anthocyanin and chlorophyll dyes on optical and photovoltaic properties of zinc oxide based dye-sensitized solar cells. Optik (Stuttg) 207:163808. https://doi.org/10.1016/j.ijleo.2019.163808

Ezike SC, Hyelnasinyi CN, Salawu MA et al (2021) Synergestic effect of chlorophyll and anthocyanin Co-sensitizers in TiO2-based dye-sensitized solar cells. Surf Interfaces 22:100882. https://doi.org/10.1016/j.surfin.2020.100882

Gunasekaran A, Sorrentino A, Asiri AM, Anandan S (2020) Guar gum-based polymer gel electrolyte for dye-sensitized solar cell applications. Sol Energy 208:160–165. https://doi.org/10.1016/j.solener.2020.07.084

Hossain MK, Pervez MF, Mia MNH et al (2017) Effect of dye extracting solvents and sensitization time on photovoltaic performance of natural dye sensitized solar cells. Results Phys 7:1516–1523. https://doi.org/10.1016/j.rinp.2017.04.011

Inbarajan K, Sowmya S, Janarthanan B (2022) Direct and soxhlet extraction of dyes from the peels of Allium cepa and its effective application in dye – sensitized solar cells as sensitizer. Opt Mater (Amst) 129:112487. https://doi.org/10.1016/j.optmat.2022.112487

Kabir F, Bhuiyan MMH, Manir MS et al (2019) Development of dye-sensitized solar cell based on combination of natural dyes extracted from Malabar spinach and red spinach. Results Phys 14:102474. https://doi.org/10.1016/j.rinp.2019.102474

Khammee P, Unpaprom Y, Thurakitseree T et al (2021) Natural dyes extracted from Inthanin bok leaves as light-harvesting units for dye-sensitized solar cells. Appl Nanosci 13:391–403

Li W, Jin G, Hu H et al (2015) Phosphotungstic acid and WO3 incorporated TiO2 thin films as novel photoanodes in dye-sensitized solar cells. Electrochim Acta 153:499–507. https://doi.org/10.1016/j.electacta.2014.12.030

Ludin NA, Al-Alwani Mahmoud AM, Bakar Mohamad A et al (2014) Review on the development of natural dye photosensitizer for dye-sensitized solar cells. Renew Sustain Energy Rev 31:386–396. https://doi.org/10.1016/j.rser.2013.12.001

Luo P, Niu H, Zheng G et al (2009) From salmon pink to blue natural sensitizers for solar cells: Canna indica L., Salvia splendens, cowberry and Solanum nigrum L. Spectrochim Acta A Mol Biomol Spectrosc 74:936–942. https://doi.org/10.1016/j.saa.2009.08.039

Mariotti N, Bonomo M, Fagiolari L et al (2020) Recent advances in eco-friendly and cost-effective materials towards sustainable dye-sensitized solar cells. Green Chem 22:7168–7218. https://doi.org/10.1039/d0gc01148g

Noor MM, Buraidah MH, Careem MA et al (2014) An optimized poly(vinylidene fluoride-hexafluoropropylene)–NaI gel polymer electrolyte and its application in natural dye sensitized solar cells. Electrochim Acta 121:159–167. https://doi.org/10.1016/j.electacta.2013.12.136

O'Regan B, Grätzel M (1991) A low-cost, high-efficiency solar cell based on dye-sensitized colloidal TiO2 films. Nature 353:737–740. https://doi.org/10.1038/353737a0

Patni N, Pillai SG, Sharma P (2020) Effect of using betalain, anthocyanin and chlorophyll dyes together as a sensitizer on enhancing the efficiency of dye-sensitized solar cell. Int J Energy Res 44:10846–10859

Prabhu TGV, Chandrasekaran J, Thangaraju D (2022) Fabrication and performance analysis of set standard natural dye-sensitized solar cell (N-DSSC) using extracted Terminalia kattapa (red), Azadirachia indica (green), and Clitoria ternatea (blue) dyes with virgin. J Mater Sci Mater Electron 33:17331–17342. https://doi.org/10.1007/s10854-022-08611-0

Prabu KM, Suguna K, Anbarasan PM, et al (2021) Sensitizers performance of dye-sensitized solar cells fabricated with Indian fruits and leaves to cite this version : HAL Id : hal-03104865 sensitizers performance of dye-sensitized solar cells fabricated with indian fruits and leaves

Rajkumar S, Kumar MN, Suguna K et al (2019) Enhanced performance of dye-sensitized solar cells using natural cocktail dye as sensitizer. Optik (Stuttg) 178:224–230. https://doi.org/10.1016/j.ijleo.2018.10.004

Ramamoorthy R, Radha N, Maheswari G et al (2016) Betalain and anthocyanin dye-sensitized solar cells. J Appl Electrochem 46:929–941. https://doi.org/10.1007/s10800-016-0974-9

Rodríguez HG, Maiti R, Avendano E et al (2017) Pigment content (chlorophyll and carotenoids) in 37 species of trees and shrubs in northeastern mexico during summer season. Pak J Bot 49(2391):2398

Sankaranarayanan S, Kathiravan I, Balasundaram J et al (2022) An analysis of the dye-sensitized solar cells fabricated with the dyes extracted from the leaves and flowers of Amaranthus cruentus. Environ Sci Pollut Res Int 29:44271–44281. https://doi.org/10.1007/s11356-022-19004-5

Sharma P, Shri R, Kumar S (2022) Phytochemical and in vitro cytotoxic screening of chloroform extract of Ehretia microphylla lamk. Stresses 2:384–394. https://doi.org/10.3390/stresses2040027

Sowmya S, Inbarajan K, Ruba N et al (2021) A novel idea of using dyes extracted from the leaves of Prosopis juliflora in dye – Sensitized solar cells. Opt Mater (Amst) 120:111429. https://doi.org/10.1016/j.optmat.2021.111429

Surana K, Bhattacharya B, Majumder S (2021) Extraction of yellow fluorescent Caesalpinia sappan L. dye for photovoltaic application. Opt Mater (Amst) 119:111347. https://doi.org/10.1016/j.optmat.2021.111347

Younis A, Riaz A, Tariq U et al (2017) Drought tolerance of leucophyllum frutescens: physiological and morphological studies reveal the potential xerophyte. Acta Sci Pol Hortorum Cultus 16:89–98. https://doi.org/10.24326/asphc.2017.6.8

Zhou H, Wu L, Gao Y, Ma T (2011) Dye-sensitized solar cells using 20 natural dyes as sensitizers. J Photochem Photobiol A Chem 219:188–194. https://doi.org/10.1016/j.jphotochem.2011.02.008